Journal of Magnetic Resonance 213 (2011) 112–118

Contents lists available at SciVerse ScienceDirect

Journal of Magnetic Resonance

journal homepage: www.elsevier.com/locate/jmr

Low-field one-dimensional and direction-dependent relaxation imaging of bovine articular cartilage

Erik Rössler, Carlos Mattea, Ayret Mollova, Siegfried Stapf*

Fachgebiet Technische Physik II/Polymerphysik, Institute of Physics, Technische Universität Ilmenau, PO Box 100 565, 98684 Ilmenau, Germany

ARTICLE INFO

Article history:
Received 8 July 2011
Revised 1 September 2011
Available online 10 September 2011

Keywords:
Low field NMR
Cartilage
Relaxometry
Anisotropy
Soft matter

ABSTRACT

The structure of articular cartilage is separated into three layers of differently oriented collagen fibers, which is accompanied by a gradient of increasing glycosaminoglycan (GAG) and decreasing water concentration from the top layer towards the bone interface. The combined effect of these structural variations results in a change of the longitudinal and transverse relaxation times as a function of the distance from the cartilage surface. In this paper, this dependence is investigated at a magnetic field strength of 0.27 T with a one-dimensional depth resolution of 50 μm on bovine hip and stifle joint articular cartilage. By employing this method, advantage is taken of the increasing contrast of the longitudinal relaxation rate found at lower magnetic field strengths. Furthermore, evidence for an orientational dependence of relaxation times with respect to an axis normal to the surface plane is given, an observation that has recently been reported using high-field MRI and that was explained by preferential orientations of collagen bundles in each of the three cartilage zones. In order to quantify the extent of a further contrast mechanism and to estimate spatially dependent glycosaminoglycan concentrations, the data are supplemented by proton relaxation times that were acquired in bovine articular cartilage that was soaked in a 0.8 mM aqueous Gd^{++} solution.

1. Introduction

The bone ends of synovial joints are covered by a thin (1–5 mm) layer of hyaline articular cartilage which allows the relative movement of the bone ends with minimal friction and distributes acting loads over a large area. In order to accomplish these tasks articular cartilage varies highly in molecular composition and organization between surface and bone interface. This depth-dependent organization is mainly defined by collagen fibrils, resulting in a fibrous ultrastructure of three histological zones in the noncalcified tissue. In layers close to the surface collagen fibrils are predominantly oriented parallel to the surface (superficial zone), they start to bend forming a mostly random orientation (transitional zone) and finally align in a perpendicular manner to the surface (radial zone) (see Fig. 1a for a schematic representation). The collagen fibrils are embedded into a multicomponent matrix consisting mostly of water and proteoglycans which are protein cores with attached glycosaminoglycans. They form a bottlebrush-like structure and can aggregate to a backbone of hyaluronic acid forming a macromolecule. Glycosaminoglycans (GAGs) are negatively charged due to the sulphated chondroitin and keratin molecules. In general, a gradient of increasing glycosaminoglycan and decreasing water concentration can be seen from the top layers to the bone interface [1].

In osteoarthritis, one of the most common degenerative joint diseases, the articular cartilage loses its functional integrity. In early stages osteoarthritis primarily alters the concentration of water and proteoglycans. Later on, damages to the collagen network occur as well as a decreasing concentration of chondrocytes [2,3]. Once a certain degree of tissue damage is reached, it is almost impossible to recapture the articular cartilage functionality without surgery. Therefore, it is desirable to diagnose osteoarthritis as early as possible.

NMR investigations which have been carried out so far have addressed predominantly the properties of articular cartilage in high magnetic fields, such as the structural variations represented by the longitudinal and transverse relaxation times. For instance, imaging studies focussing on orientation-dependent contrast and pressure influence [4,5] were carried out, while spectroscopic and diffusion measurements elucidated the effect on molecular and transport properties [6]. Combinations of spectroscopic techniques and microimaging were applied for assessing order and its dependence on physiological conditions [7,8]. Low-field applications, however, are comparatively scarce: In an early work, the superiority of T_1 vs. T_2 contrast in cartilage imaging at 0.15 T was already pointed out [9]; dedicated devices for extremities have been presented [10], and routines for osteoarthritis prediction at 0.18 T were discussed [11]. Different aspects of low-field and high-field cartilage imaging are reviewed in [12,13]. For a similar system of rather high molecular order, bovine Achilles tendon,

* Corresponding author.
E-mail address: siegfried.stapf@tu-ilmenau.de (S. Stapf).

1090-7807/$ - see front matter © 2011 Elsevier Inc. All rights reserved.
doi:10.1016/j.jmr.2011.09.014

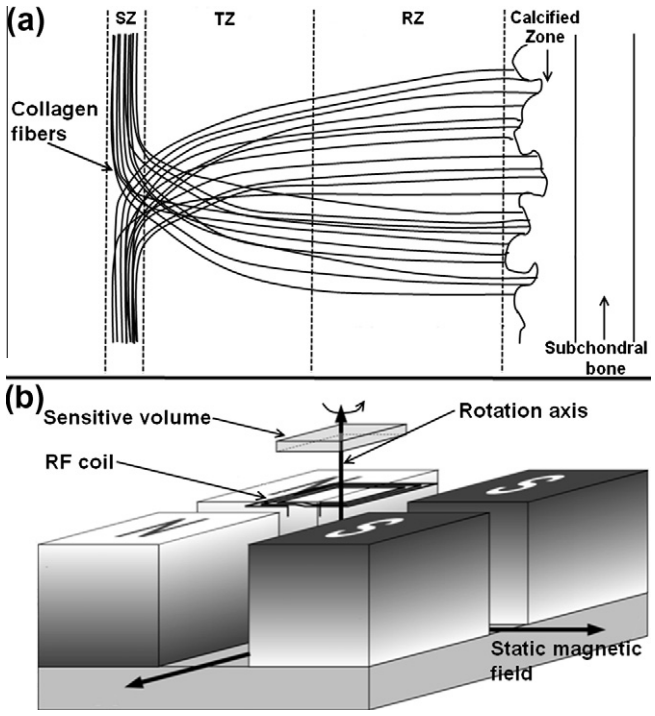

Fig. 1. (a) Sketch of cartilage structure. The cartilage itself is approximated by a leaf-like structure with fiber orientations predominantly parallel to the joint surface (superficial zone), perpendicular to the bone surface (radial zone) and mixed orientations in between (transition zone). Calcified zone and subchondral bone are within the accessible volume of the cartilage samples in this study. (b) Visualization of the NMR scanner with directions of magnetic field and sample rotation axis. The field gradient points upward, i.e. normal to the plane of the rf coil.

anisotropy of both T_2 [14] and diffusion [15] were reported using a portable low-field sensor.

In this contribution, we report about experiments carried out at a low magnetic field strength (0.27 T), taking advantage of the increased contrast of the longitudinal relaxation rate towards lower Larmor frequencies.

2. Experimental procedure

Samples of bovine articular cartilage taken from fresh hip and stifle joints of a femur bone were cut in pieces of approximately 6 by 8 mm and roughly 8 mm in thickness including the bone itself; they were placed in physiological saline solution (PBS) in a refrigerator at 6.8 °C for 24 h. PBS is an isotonic water-based buffer solution containing mostly sodium chloride and phosphate as well as small amounts of potassium chloride and phosphate, which helps to maintain a constant pH value around 7.4. Each sample was removed from the physiological solution 3 h prior to the measurement, put in a Petri dish and kept unclosed in the refrigerator to remove excess surface moisture. Afterwards the sample was wrapped in cling film.

The spatially resolved experiments were performed using the stray field of a single sided NMR spectrometer (Profile NMR-MOUSE, ACT GmbH, Germany) with a ^{1}H resonance frequency of 11.7 MHz (corresponding to a magnetic field strength of 0.27 T) providing a time-constant magnetic field gradient of 11.5 T/m in the sensitive volume. The magnet and sample are kept at room temperature within 0.5 °C. The temperature of the magnet was monitored during the whole process, possessing a variation of ±0.5 °C. At the position of the sample, a minor increase in the temperature was detected due to the heating of the RF coil. This heating was well below 0.5 °C and did not significantly affect the relaxation process.

Profiles were obtained by moving the magnet relative to the sample which was oriented with the cartilage surface facing the receiver coil of 10 × 10 mm area. Due to the strong field gradient, only a thin slice at a distance of several mm from the magnet surface is excited and contributed to the signal. Experiments were carried out as CPMG trains with a pulse separation of either 87.5 μs or 66.5 μs using a 180° pulse length of 3.5 μs; for these parameters, the thickness of the excited slice was 50 μm or 100 μm, respectively [16]. The step size of the stepping motor was set accordingly to either 50 μm or 100 μm. From the total of typically 1024 echoes acquired, the transverse relaxation times T_2 were fitted. Note that due to the heterogeneity of the magnetic field, the apparent relaxation time of a free water sample is obtained as approximately 200 ms in contrast to its true value of 2–3 s; although the actual value of T_2 in this study is of less importance than the contrast between different layers and orientations, we nevertheless wish to state that the values measured for the discussed systems indeed represent, with minimal deviation, the true values in the absence of magnetic field gradients. Also, the spin-locking effect, which would lead to a signal decay component governed by $T_{1\rho}$, can be considered negligible since rf power is present during a maximum of 5% of the sequence time. Data for the upper layers (superficial, transition and radial zones) could be fitted successfully by monoexponential decay functions, i.e. no significant second contribution was identified, in agreement with previous high-field investigations [17]. Decays in the calcified zone and within the subchondral bone, however, required biexponential fits.

Longitudinal relaxation times (T_1) were obtained by using a saturation recovery sequence followed by a CPMG train for increasing the signal intensity; the first 512 echoes of the train were added. These data could always be fitted using a monoexponential function.

Orientation dependent measurements were carried out by rotating the sample in steps of 15° about the axis perpendicular to the receiver coil, this axis being also perpendicular to the B_0 direction (see Fig. 1b). In order to prevent a bias from sample drying, angular positions were set in random order, and the initial position was measured again at the end of the experiment.

For measurements including the contrast agent, a full profile of a cartilage sample was first completed, the sample was then placed in 0.8 mM $Gd(DTPA)^{2-}$ solution for 24 h, and the same sample was measured, after removing excess water from the surface, in the exact position as before.

Frequency-dependent measurements of the longitudinal relaxation time, $T_1(\omega)$, were carried out at a commercial field-cycling relaxometer (Stelar s.r.l., Mede, Italy) with Larmor frequencies $\omega/2\pi$ in the range of 10 kHz–20 MHz at room temperature; typically 8 scans were accumulated for each frequency. The resulting decay curves were fitted as exponentials (see [18] for technical details).

3. Results and discussions

3.1. Transverse relaxation times

The dependence of the transverse relaxation time, T_2, on depth is shown in Fig. 2 where the hip joint and the stifle joint of a bovine femur bone are compared to each other. In both samples, a particularly short T_2 value is identified at the cartilage surface, increasing towards a maximum value almost twice as high at a depth of approximately 600 μm, before decreasing again towards a second minimum. This minimum clearly corresponds to the calcified zone which possesses a smaller concentration of water that is considerably more restricted in mobility. Nevertheless, the measured T_2 values of between 16 ms and 25 ms still indicate a relatively large

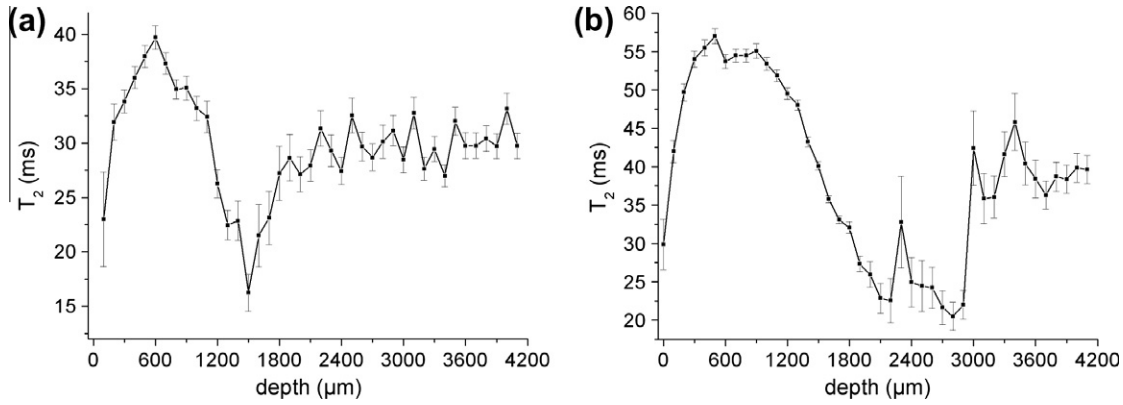

Fig. 2. Transverse relaxation time T_2 as a function of tissue depth for bovine articular cartilage (left: hip joint, right: stifle joint). Data were acquired by a CPMG sequence at a spatial resolution of 100 μm. The repetition time was 3000 ms, and the number of accumulations was 128 (hip joint) and 64 (stifle joint), respectively.

mobility of the remaining water molecules. The calcified zone appears to be of varying thickness, i.e. an almost constant T_2 is found within a region of about 1 mm thickness in the stifle joint, while T_2 increases more gradually with growing depth in the hip joint. A different actual thickness of the calcified zones can be concluded, but an influence of a different curvature of both regions, leading to overlap of signals within the sensitive volume of the sensor, cannot be ruled out as well. For tissue extending further away from the surface, relaxation times increase once more, the signal originates from fluid inside the subchondral bone. Note that only the long component of a biexponential fit is shown in Fig. 2; the short component typically in a range of 0.6–1.0 ms was contributing with a weight fraction of about 60–70%, but no attempt was made to quantify this contribution since the focus of this work was on the cartilage tissue.

The increase and subsequent decrease of T_2 from the surface towards the calcified zone has repeatedly been reported in the literature, e.g. for canine articular cartilage at high magnetic fields (7 T) [19]. Although a direct comparison of tissue from different joints in different mammals is impossible, the trend appears to be universal:

Transverse relaxation times, and thus water mobility, are lowest immediately at the surface, an observation that has been made for tissue samples embedded in buffer solution [20], so that superficial drying due to evaporation cannot be made fully responsible for this effect. Nevertheless, for the experiments shown in this study, drying during the experiment could not fully be prevented, so that the actual gradient in T_2 may be somewhat smaller than the range observed, despite the fact that the ratio between minimum and maximum T_2 values within the cartilage agrees with previous studies. The increase in T_2, maximum of T_2 and its subsequent decrease towards the calcified zone have been interpreted as superficial, transitional and radial zone, respectively [21]. Although no sharp boundaries are to be expected and the size of each zone depends on the cartilage thickness as well as the location it was taken from, the transition between the three cartilage zones can be clearly seen.

When comparing the depth-dependence of T_2 with values in the literature, the ubiquitous direction dependence has to be taken into account: note that in our experiments, the direction of the external magnetic field was *parallel* to the cartilage surface (see Fig. 1b). In a conventional medical MRI scanner, the external magnetic field would be *perpendicular* to the cartilage surface in most of the main joints.

3.2. Longitudinal relaxation times

Contrary to T_2, the longitudinal relaxation time T_1 was reported to *not* show significant variation across cartilage tissue when measured at high magnetic field strengths [19,22]. At a field strength of 0.27 T, however, a pronounced variation of T_1 is found, as is demonstrated in Fig. 3. For both the hip joint and the stifle joint, the systematic behavior of T_1 across the cartilage region approximately follows that of the T_2 dependence. An increase from the surface towards a maximum at about 600 μm depth is followed by a subsequent continuous decrease towards the calcified region, from which it remains constant or increases weakly towards the subchondral bone, at variance to the T_2 behavior in this region which

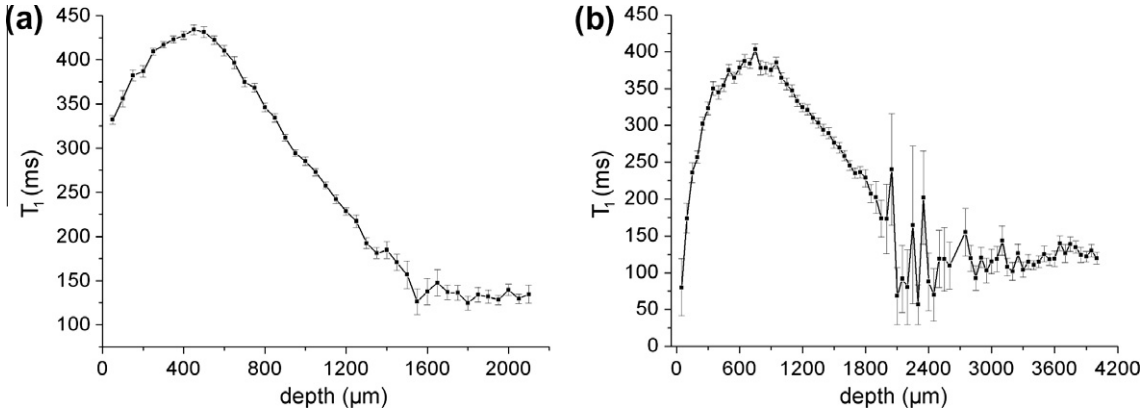

Fig. 3. Longitudinal relaxation time T_1 as a function of tissue depth for bovine articular cartilage (left: hip joint, right: stifle joint). Data were acquired by a saturation recovery sequence followed by a CPMG train for increasing signal-to-noise ratio. The spatial resolution has been 50 μm. The repetition time was 2500 ms, and the number of accumulations was 64 (hip joint) and 32 (stifle joint), respectively.

features a more pronounced increase below the calcified region. Note that experiments were carried out at different samples cut from the same joints, so that an exact match of tissue dimensions is not expected, but they have indeed been very similar to each other. Repeated experiments with further samples taken from the same or different bovine joints do follow the same behavior and show similar absolute T_1 values. In Fig. 3, the maximum variation of T_1 across the sample is between a factor of 3 and 4, where the immediate top layer of the stifle joint has not been considered due to large fitting errors. These are possibly influenced by sample drying during T_1 experiments, since the profile was measured starting from the bone and moving towards the cartilage surface, and took considerably longer than T_2 measurements. Based on the separation of the sample into three cartilage zones, the behavior of T_1 across these zones can well be identified in Fig. 3. At the field strength used in this study, T_1 appears to be a superior parameter for characterization across the cartilage tissue and beneath it, since the dynamic range of the T_1 values is larger than that of T_2 and the fitting error is significantly lower, which indicates a smaller spatial variation across the sensitive volume in each experiment. Much stronger variations are seen in the calcified zone, in particular in the stifle joint, which are accompanied by large fitting errors and are also a consequence of the smaller signal intensity (see below).

The more pronounced dependence of T_1 towards lower magnetic field strengths has its origin in the dipolar relaxation mechanism of the protons and the related correlation times. From the monoexponential behavior it can be concluded that protons either exist in a single, motionally restricted phase (because of the T_1 value being considerably reduced compared to bulk water), or are in fast exchange between two or more separate phases, such as free and bound water. If for all of these phases, the molecular motion can be approximated by isotropic rotation with a characteristic time τ so that $\omega\tau \ll 1$, relaxation theory requires a field-independent relaxation rate $1/T_1$ that is proportional to τ [23,24]. Any more complex correlation function, involving reorientation times on the order of ω^{-1} or slower, must result in a field dependent, and thus frequency dependent, relaxation time; indeed, such a frequency dependence has regularly been observed for water in biological tissue, including proteins, muscle tissue and live leeches [18]. Fig. 4 shows the frequency dependence of protons in a cartilage sample cut from the bone; the plotted T_1 correspond to averages over the whole tissue, i.e. averages over the continuous distribution of T_1 values as shown in Fig. 3. The frequency dependence can be approximated by a power law of $T_1 \sim \omega^{0.23}$ from the lowest frequencies upward, with a slightly more pronounced field dependence in the MHz region. There is indeed evidence for a frequency dependence that is different for the individual layers of the cartilage tissue, which would explain the variation found at 0.27 T and its essential absence at 7 T [19]. Earlier results on relaxation times in the rotating frame, $T_{1\rho}$, which have been found to depend on position as well as on the distribution of GAG concentrations, confirm that contrast may exist even at very low Larmor frequencies [25]. Further research is currently carried out on quantifying the relaxation dispersion within the individual zones of cartilage tissue.

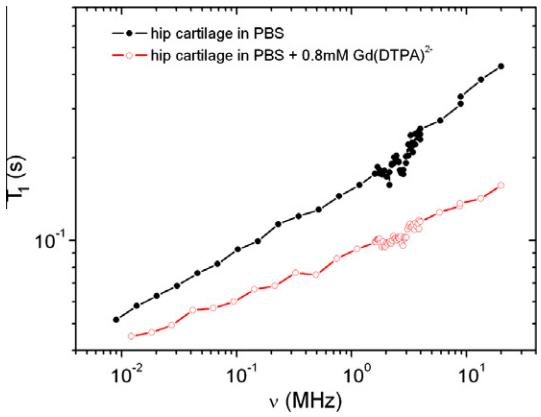

Fig. 4. Frequency-dependent relaxation time T_1 obtained by field-cycling relaxometry. Data represent measurements before and after the addition of a 0.8 mM $(Gd\text{-}DTPA)^2$ aqueous solution. Shorter T_1 values at frequencies of 2.2 and 2.9 MHz correspond to cross-relaxation effects of protons with ^{14}N-nuclei in the amide groups.

Note the occurrence of quadrupolar dips around 2.2 and 2.9 MHz, which are a consequence of ^{1}H–^{14}N cross relaxation of protons with nitrogen nuclei in amide groups of the immobilized collagen and/or GAG macromolecules [26,27]. The depth of these dips provides access to the concentration and the degree of motional anisotropy of H–N pairs in the sample.

3.3. Signal intensity

Results of T_2 and T_1 distributions across the cartilage region and into the subchondral bone qualitatively match previously reported T_2 dependences, but samples in this study have not been immersed in liquid during the experiment so that drying due to water evaporation may exist despite their sealing by a cling film. In an attempt to estimate the influence of drying, the signal intensity of the sample has been reconstructed from the layer-dependent measurements (see Fig. 2) by integrating the signal intensity of the 2nd to 5th echoes, which are negligibly affected by transverse relaxation. The profile shown in Fig. 5 corresponds to the total signal of mobile protons, i.e. predominantly water and proteoglycans. While the signal decreases towards the surface, possibly indicating drying of the sample, it remains constant between about 600 and 1600 μm, where T_2 and T_1 variations are obvious in corresponding measurements. Signal intensity then decreases towards the calcified zone and slightly increases again within the subchondral bone, with about half the signal intensity of that in the center of the cartilage region. Note that a possible mismatch of the sensitive volume with the sample surface, i.e. the fact that the topmost slice may be partially outside the sample, is another reason for a reduced signal intensity (leftmost point in Fig. 5). The relaxation times measured are, however, unaffected by this partial-volume effect.

An indirect proof of the effect of drying on the measurement parameters is the evolution of the longitudinal relaxation as a function of time; Fig. 6 shows this parameter, taken at a depth of 150 μm, in its evolution during 16 h. This period much exceeds the duration of a profile experiment, which is approximately

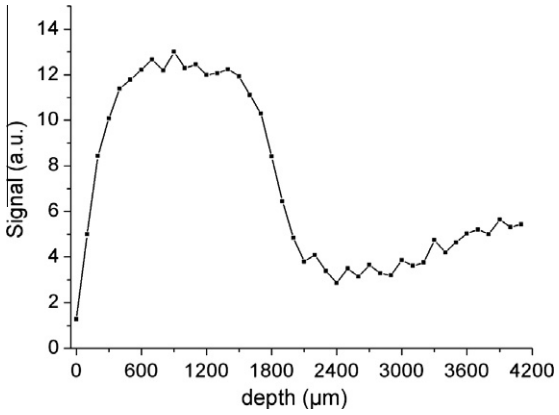

Fig. 5. Signal intensity obtained from adding the 2nd to 5th echoes of the measurement of Fig. 2b (stifle joint).

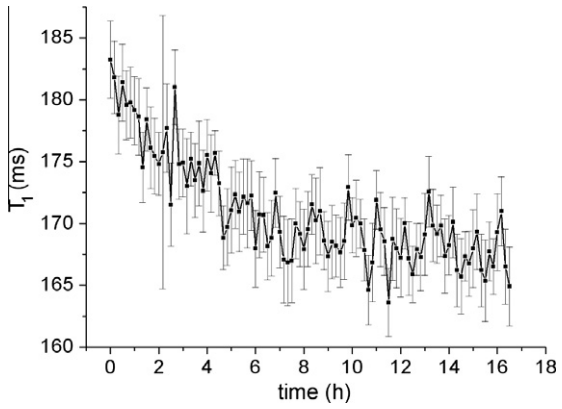

Fig. 6. Longitudinal relaxation time T_1 at a depth of 150 μm for bovine articular cartilage (stifle joint). Data show the evolution of T_1 in the same depth over the course of 16 h.

3.5 h for a T_1 profile and 1 h for a T_2 profile. During this period, a decay of T_1 of 8% with a time constant of about 5 h is observed, which clearly indicates that the considerable variation of T_1 across the sample is not significantly influenced by time-dependent changes during the time of the experiments.

3.4. Relaxation times with contrast agent

$(Gd\text{-}DTPA)^{2-}$ has been applied as a common relaxation agent in medical imaging to, for instance, follow the fluid transport of an injection bolus, or to quantify local water concentrations because only water molecules in exchange with a hydration shell around the ions are affected. Due to the timescale of this molecular exchange, a weak frequency dependence of water protons in aqueous $(Gd\text{-}DTPA)^{2-}$ solution has been reported [28]. Applying a contrast agent to cartilage tissue provides a handle to quantify the actual water concentration, and indirectly also GAG concentration, important parameters for assessing tissue status and for identifying degenerative changes in cartilage. The application of physiologically accepted concentrations of $(Gd\text{-}DTPA)^{2-}$, and the comparison of relaxation times before and after application, has been suggested as a means to quantify GAG concentration [29], and good agreement with chemometric results has been achieved [1].

Fig. 7a compares the longitudinal relaxation times for one particular hip joint sample, where a measurement without contrast agent was followed by a period of storage in a 0.8 mM aqueous $(Gd\text{-}DTPA)^{2-}$ solution (see Section 2) and a second experiment with identical conditions. While relaxation times in the transition zone were reduced by almost two thirds, the reduction becomes less pronounced towards the calcified zone; the relative change is shown in Fig. 7b.

Ref. [29] provides a recipe for determining GAG concentration from the difference of relaxation rates under the assumption of a known counter-ion concentration. If this procedure is followed, the profile of GAG concentrations shown in Fig. 7c is obtained. A strong increase until a depth of 750 μm is clearly visible, afterwards more fluctuations occur and the increase is weaker. This result confirms the profile obtained in [1], where a distinct concentration gradient is found by NMR as well as chemometric methods.

Note that no significant influence of the contrast agent on transverse relaxation times was observed. Frequency dependence of

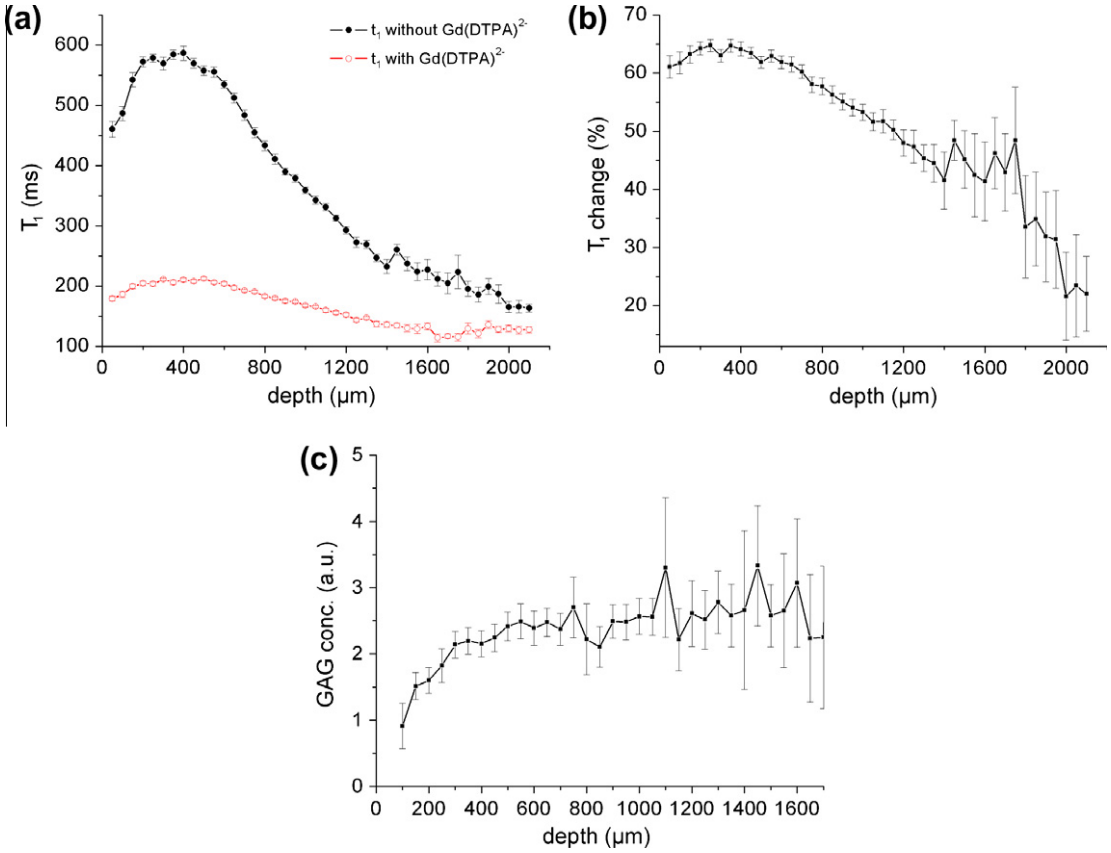

Fig. 7. (a) Longitudinal relaxation time T_1 as a function of tissue depth for bovine articular cartilage (hip joint). Data were acquired by a saturation recovery sequence followed by a CPMG train for increasing signal-to-noise ratio. The spatial resolution has been 50 μm. The repetition time was 2500 ms, and the number of accumulations was 32. The red (bottom) curve corresponds to the results after addition of a 0.8 mM $(Gd\text{-}DTPA)^2$ aqueous solution. (b) Relative change of T_1 as a function of tissue depth (computed from the data in (a)). (c) GAG concentration as a function of tissue depth, computed by applying the formalism of [29].

longitudinal relaxation times, on the other hand, was altered by the addition of the $(Gd\text{-}DTPA)^{2-}$ solution, see Fig. 4. Relaxation rates are obtained from a sum of the rates of the water-containing samples and the solution with contrast agent, the latter contributing a higher relaxation rate above a Larmor frequency of about 4 MHz. This has also the effect of significantly reducing the prominence of the quadrupolar dips which are unrelated to the proton–electron cross-relaxation of the Gd-compound. It can be concluded that, while the application of $(Gd\text{-}DTPA)^{2-}$ is a suitable method for quantifying spatially dependent GAG concentration, the range of T_1 values as a function of depth and magnetic field strength becomes reduced so that, apart from a certain gain in experimental duration due to the reduced repetition times, the use of contrast agents does not *per se* facilitate the assessment of cartilage tissue at low field.

3.5. Angular dependence

In recent literature, the dependence of the transverse relaxation time on the sample orientation with respect to the external magnetic field was discussed in detail [30,31]. Such a dependence is expected due to the known preferential orientation of the collagen fibers in the three different cartilage zones; on the other hand, relaxation of water molecules that are experiencing this orientation by molecular motion in an anisotropic environment can be employed as probes for models describing this tissue property, and can serve as indicators for degenerative processes that can affect this order. Of the three possible rotation axes investigated in [30], only one could be studied in this work, because of the geometry of the sensor that allows measurement only within one two-dimensional layer.

In Fig. 8a and b, the angular variation of T_2 and T_1 data, respectively, are compared at a depth of 150 μm in a bovine stifle joint prepared with 0.8 mM aqueous $(Gd\text{-}DTPA)^{2-}$ solution. Similar experiments were carried out with a number of joints but no statistically significant variation was identified; in particular, samples without contrast agent showed only small and unsystematic variations. In order to test the significance of the variation of the presented results, the autocorrelation function of angles has been obtained and is shown in Fig. 8c and d. This function is defined as:

$$G(\phi) = \frac{\langle P(\delta)P(\delta+\phi)\rangle}{P(\delta)^2},$$

where the quantity $P(\delta)$ corresponds to the relaxation time at a given angle ϕ relative to the external magnetic field.

The variation of T_2 with angle is statistically significant and shows a periodicity of $(75 \pm 5)^\circ$. Within the transition zone, where these data have been determined, the bundle arrangement of collagen fibers has been reported to generate a variation with a periodicity of about 90° [30]. This behavior is also indentified in this study. The relatively weakly pronounced variation can be explained by the fact that, apart from vertical averaging over a slice thickness of 50 μm, lateral averaging over the whole width of the cartilage sample of 6 by 8 mm occurs. A global orientation over such a large dimension is unrealistic, so that some averaging of locally oriented fiber bundles does inevitably occur during the experiment.

Note that no significant variation of T_1 was found, as is seen in Fig. 8a and c. Since longitudinal relaxation is proportional to the same angle-dependent functions as T_2, such a dependence cannot a priori be ruled out, although it has not been reported yet. Further studies on smaller samples are currently been carried out to quantify T_1 variations.

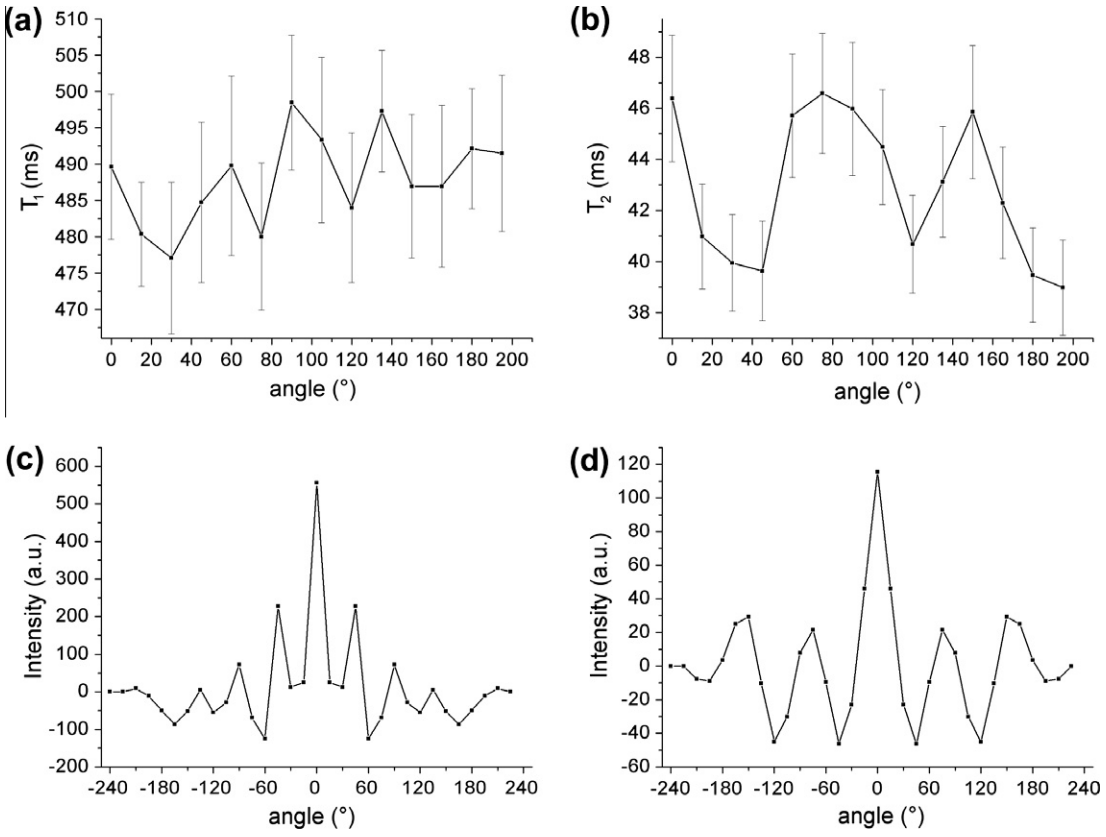

Fig. 8. (a and b) Dependence of T_1 and T_2 on the angle between B_0 and a horizontal line through the initial sample position (hip sample). The spatial resolution has been 50 μm. The repetition time was 1800 ms, and the number of accumulations was 32. (c and d) Autocorrelation function of angle-dependent relaxation time measurements for T_1 (left) and T_2 (right).

4. Conclusions

The feasibility to obtain relaxation parameter maps across articular cartilage samples at low magnetic field strength with a portable device was demonstrated for the example of bovine articular cartilage samples of 6 by 8 mm in size. Despite a possible curvature of the samples themselves, the three-layer structure known from the literature could be reproduced satisfactorily. While transverse relaxation times at a field strength of 0.27 T show a similar range as those reported at 7 T, the contrast of the longitudinal relaxation times is considerably larger at low fields, which suggests their potential use for systematic investigations of diseased cartilage. The use of a Gd contrast agent is a suitable method to estimate water and/or glycosaminoglycan concentrations and bears the potential to visualize, on a low-field scanner, anomalities which do occur in some types of degenerative tissue diseases (osteoarthritis, articular gout and rheumatism). Finally, a weakly pronounced angular dependence about the cartilage's surface normal axis is found, the main reason for this effect being much smaller than previously reported [30] is probably the fact that the collagen bundle orientations are averaged over a large area, while there is reason to assume that local preferential orientations are restricted to much smaller domain sizes.

This work represents a feasibility study and thus a first step towards a simple, and possibly routine, ex vivo characterization modality for cartilage tissue. The current total experimental time of roughly 1 h for a T_2 profile and 3.5 h for a T_1 without contrast agent can possibly be reduced by employing somewhat stronger magnetic fields or more sensitive receiver circuits. An improved version of the experiment using a smaller pick-up coil, thus providing a better filling factor even with smaller samples, at the same time allowing a less curved sample geometry, is currently under way. On the other hand, the proposed and partially observed higher sensitivity of the longitudinal relaxation time at this field strength can be increased further if experiments were carried out at lower field strengths. The optimum choice of contrast agents, which may be used as a marker to GAG degeneracies and other types of diseased tissue, depends on the actual Larmor frequency used, with $(\text{Gd-DTPA})^{2-}$ (Magnevist) representing only a first, straightforward and commercially available option. Logical improvements of the presented approach are techniques towards order-sensitive multipulse methods and the encoding of diffusion parameters. Finally, further field-cycling experiments quantifying the relaxation dispersion within the individual cartilage zones will be carried out.

Acknowledgments

We are grateful to Yang Xia for invaluable discussions throughout the course of this project. We acknowledge the contribution of the Naturfleisch GmbH Rennsteig, Oberweissbach company for providing us with fresh bone samples. E. Rössler gratefully appreciates the support of S. Ghoshal.

References

[1] Y. Xia, S. Zheng, A. Bidthanapally, Depth-dependent profiles of glycosaminoglycans in articular cartilage by μMRI and histochemistry, J. Magn. Reson. Imaging 28 (2008) 151–157.
[2] J. Hesse, W. Mohr, W. Hesse, Morphologische Veränderungen in frühen Stadien der Arthrose, Orthopädie 19 (1990) 16–27.
[3] H. Lorenz, W. Richter, Osteoarthritis: cellular and molecular changes in degenerating cartilage, Prog. Histochem. Cytochem. 40 (2006) 135–163.
[4] W. Gründer, M. Kanowski, M. Wagner, A. Werner, Visualization of pressure distribution within loaded joint cartilage by application of angle-sensitive NMR microscopy, Magn. Reson. Med. 43 (2000) 884–891.
[5] J.D. Rubenstein, J.K. Kim, I. Morava-Protzner, P.L. Stanchev, R.M. Henkelman, Effects of collagen orientation on MR imaging characteristics of bovine articular cartilage, Radiology 188 (1993) 219–226.
[6] D. Huster, J. Schiller, L. Naji, J. Kaufmann, K. Arnold, NMR studies of cartilage – dynamics, diffusion, degradation, molecules in interaction with surfaces and interfaces, Lect. Notes Phys. 634 (2004) 465–503.
[7] H. Shinar, Y. Seo, K. Ikoma, Y. Kusaka, U. Eliav, G. Navon, Mapping the fiber orientation in articular cartilage at rest and under pressure studied by 2H double quantum filtered MRI, Magn. Reson. Med. 48 (2002) 322–330.
[8] K. Keinan-Adamsky, H. Shinar, S. Shabat, Y.S. Brin, M. Nyska, G. Navon, 23Na and 2H magnetic resonance studies of osteoarthritic and osteoporotic articular cartilage, Magn. Reson. Med. 64 (2010) 653–661.
[9] M.E. Adams, D.K.B. Li, J.P. McConkey, R.G. Davidson, B. Day, C.P. Duncan, V. Tron, Evaluation of cartilage lesions by magnetic resonance imaging at 0.15 T – comparison with anatomy and concordance with arthroscopy, J. Rheumatol. 18 (1991) 1573–1580.
[10] H. Yoshioka, S. Ito, S. Handa, S. Tomiha, K. Kose, T. Haishi, A. Tsutsumi, T. Sumida, Low-field compact magnetic resonance imaging system for the hand and wrist in rheumatoid arthritis, J. Magn. Reson. Imaging 23 (2006) 370–376.
[11] A.A. Qazi, J. Folkesson, P.C. Pettersen, M.A. Karsdal, C. Christiansen, E.B. Dam, Separation of healthy and early osteoarthritis by automatic quantification of cartilage homogeneity, Osteoarthritis Cartilage 15 (2007) 1199–1206.
[12] T.M. Link, R. Stahl, K. Woertler, Cartilage imaging: motivation, techniques, current and future significance, Eur. Radiol. 17 (2007) 1135–1146.
[13] B. Ostendorf, E. Edelmann, H. Kellner, A. Scherer, Low-field magnetic resonance imaging for rheomatoid arthritis, Z. Rheumatol. 69 (2010) 79.
[14] R. Haken, B. Blümich, Anisotropy in tendon investigated in vivo by a portable NMR scanner, the NMR MOUSE, J. Magn. Reson. 144 (2000) 195–199.
[15] M. Klein, R. Fechete, D.E. Demco, B. Blümich, Self-diffusion measurements by a constant-relaxation method in strongly inhomogeneous magnetic fields, J. Magn. Reson. 164 (2003) 310–320.
[16] B. Blümich, J. Perlo, F. Casanova, Mobile single-sided NMR, Prog. Nucl. Magn. Reson. Spectrosc. 52 (2008) 197–269.
[17] Y. Xia, Magic-angle effect in magnetic resonance imaging of articular cartilage: a review, Invest. Radiol. 35 (2000) 602–621.
[18] R. Kimmich, E. Anoardo, Field-cycling NMR relaxometry, Prog. Nucl. Magn. Reson. Spectrosc. 44 (2004) 257–320.
[19] Y. Xia, Relaxation anisotropy in cartilage by NMR microscopy (μMRI) at 14-μm resolution, Magn. Reson. Med. 39 (1998) 941–949.
[20] Y. Xia, J.B. Moody, H. Alhadlaq, Orientational dependence of T2 relaxation in articular cartilage: a microscopic MRI (μMRI) study, Magn. Reson. Med. 48 (2002) 460–469.
[21] Y. Xia, T. Farquhar, N. Burton-Wurster, G. Lust, Origin of cartilage laminae in MRI, J. Magn. Reson. Imaging 7 (1997) 887–894.
[22] R.M. Henkelmann, G.J. Stanisz, J.K. Kim, M.J. Bronskill, Anisotropy of NMR properties of tissues, Magn. Reson. Med. 32 (1994) 592–601.
[23] A. Abragam, The Principles of Nuclear Magnetism, Oxford University Press, London, 1961.
[24] R. Kimmich, NMR – Tomography, Diffusometry, Relaxometry, Springer Verlag, Berlin, 1997.
[25] S.V.S. Akella, R.R. Regatte, A.J. Gougoutas, A. Borthakur, E.M. Shapiro, J.B. Kneeland, J.S. Leigh, R. Reddy, Proteoglycan-induced changes in T1rho-relaxation of articular cartilage at 4T, Magn. Reson. Med. 46 (2001) 419–423.
[26] R. Kimmich, F. Winter, W. Nusser, K.-H. Spohn, Interactions, Interactions and fluctuations deduced from proton field-cycling relaxation spectroscopy of polypeptides, muscles, DNA and algae, J. Magn. Reson. 68 (1986) 263–282.
[27] E.P. Sunde, B. Halle, Mechanisms of 1H–14N cross-relaxation in immobilized proteins, J. Magn. Reson. 203 (2010) 257–273.
[28] L. Banci, I. Bertini, C. Luchinat, Nuclear and Electron Relaxation: The Magnetic Nucleus-Unpaired Electron Coupling in Solution, Wiley-VCH, 1991.
[29] A. Gillis, M. Gray, D. Burstein, Relaxivity and diffusion of Gadolinium agents in cartilage, Magn. Reson. Med. 48 (2002) 1068–1071.
[30] S. Zheng, Y. Xia, The collagen fibril structure in the superficial zone of articular cartilage by μMRI, Osteoarthritis Cartilage 17 (2009) 1519–1528.
[31] S. Zheng, Y. Xia, F. Badar, Further studies on the anisotropic distribution of collagen in articular cartilage by μMRI, Magn. Reson. Med. 65 (2009) 656–663.